https://doi.org/10.36375/prepare_u.iiche.a379

Synthesis of multifunctional Ag NPs by using different plants

Rebika Baruah[a,b*], Archana Moni Das[a,b]

[a]*CSIR-North East Institute of Science and Technology, Jorhat-785006, Assam, India*

[b]*Academy of Scientific and Innovative Research (AcSIR), Ghaziabad-201002, India*

Abstract

Green synthesis of metal nanoparticles by using plant extracts is an environment-friendly, cost-effective and sustainable method. In our experiment, plant extracts of *Livistona jekinsiana* and *Lasia spinosa* were used in the synthesis of Ag NPs for the first time. Due to the high antioxidants contained and the traditional therapeutic applications of the mentioned plants, they were selected as ideal reducing and capping agents in the synthesis of Ag NPs. The synthesis of the Ag NPs was preliminarily confirmed by UV- Visible spectra of the synthesized NPs. The Fourier transform infrared (FTIR) spectra indicated the presence of -OH, C=C, -CN, -CH, etc. functional groups of phytocompounds on the surface of NPs. XRD patterns of Ag NPs revealed the FCC structure of the Ag NPs. FESEM and HRTEM micrographs determined the spherical shape and uniform size of the Ag NPs. EDX analysis confirmed the purity of Ag NPs. Higher negative values of zeta potential revealed the higher stability of the NPs. The NPs exhibited potential antimicrobial activity against Gram-positive bacteria *Staphylococcus aureus* (ATCC 11682), Gram-negative bacteria *Escherichia coli* (ATCC 11229), *Pseudomonas aeruginosa* (MTCC 2582), and fungi *Candida albicans* (MTCC 3017). Ag NPs also showed antioxidant activity, anti-inflammatory activity, and drug delivery ability with good results. The photocatalytic activity of Ag NPs was examined by the degradation of nitro compounds in the presence of sunlight. The kinetics of the photodegradation and reusability of the Ag NPs were also studied.

Keywords: Green synthesis; Ag NPs; Biomedical application; Catalytic Activity

1. Introduction

Nanoparticles are fruitful products in the current generation. Nanotechnology deals with particles in the dimensions of 1-100 nm[1,2]. Nanoparticles (NPs) covered all the aspects of daily life e.g., medicine, cosmetics, food, electronics, automobiles, environmental remediation, drug delivery, etc.[1]. NPs can be synthesized by both chemical and physical methods. Conventional methods have a lot of disadvantages like the use of harmful chemicals, high pressure, and temperature, costly and space-consuming sophisticated equipment, and time-consuming methods. Therefore, a new alternative method should be required to synthesize such beneficial materials[3]. Plant extracts are the ideal replacement in the synthesis of NPs that requires no extra chemicals and equipment. Green synthesis of NPs by the plant extracts overcomes all the obstacles that arise from the conventional methods[3,4].

Ag NPs are the most useful NPs among the noble metal NPs. Due to their unique properties, like high surface-to-volume ratio, extra small size, and high surface plasmon resonance, they have versatile applications in several fields, e.g., environmental remediation, biomedical, food technology, optical, and electrical fields[5]. Many plants are used in the synthesis of Ag NPs. *Alpinia nigra* fruits mediated Ag NPs[6], jasmine flower extract synthesized Ag NPs[7], *Artocarpus heterophyllus* and *Azadirachta indica* mediated Ag NPs[1], *Citrus medica*, *Tagetes lemmonii*, and *Tarenna asiatica* assisted Ag NPs[8], onion peels mediated Ag NPs[9,] etc. Polyphenolic compounds present in the plant extracts reduced Ag+ ions to Ag(0) NPs and stabilized them by capping around the NPs[2]. In our study, *Livistona jekinsiana* and *Lasia spinosa* were selected to synthesize Ag NPs. *Livistona jekinsiana* belongs to the Arecaceae family and is found on the Indian continent. The plant possesses anticancer, and antioxidant activities and uses in the lowering of uric acid levels in blood[10]. *Lasia spinosa* belongs to *the* Araceae family and the leaves and rhizomes of this plant are used in Ayurvedic medicine. *Lasia spinosa* has a lot of biological activities like antidiabetic, antibacterial, antioxidant, anti-analgesic, anthelmintic, and anticestodal activity and the plant is also used traditionally in cholic, rheumatism, and intestinal disorders[11].

Water is polluted by many industrial effluents like dyes, pesticides, manure, and waste medicines[12]. Among them, nitro compounds cause serious detrimental effects on the water bodies. They decrease the amount of oxygen in the water and deteriorated aquatic life. Scavenging of these non-biodegradable, carcinogenic, and mutagenic organic pollutants in a simple and mild conditions is an urgent need[12]. Photodegradation is one of the efficient methods to degrade organic pollutants and fulfill all the criteria of a simple method in green conditions. This method minimizes the extra use of chemicals, time, and byproducts, and degraded the pollutants into mineral acids like CO_2 and H_2O[12]. Ag NPs successfully degrade the dyes due to their high surface area. The high surface area offered a large number of active sites to catalyze the degradation. High surface plasmon resonance of Ag NPs makes them suitable to catalyze the degradation of dyes under visible light[13]. Therefore, in our study 2-nitro aniline was degraded in presence of Ag NPs under solar irradiation. In the literature, many NPs were used in the reduction of nitro compounds to amino compounds. E.g., Ag NPs@cellulose polymer paper[12], lignin mediated Ag NPs[14], Pt@Cu/TiO_2 nanocomposite[15], *Camellia japonica* leaf extract mediated Ag NPs[16], Ag/ZnO nanoflowers[17], etc..

Multidrug-resistant pathogens cause severe problems in the medicinal field. Therefore, the replacement of traditional antibiotics with the microbes-resistant drug is very essential for humans[18]. Metal NPs, especially Ag NPs is very ideal candidates for this replacement. Ag is used in medicine since ancient times. Along with the bactericidal effect of Ag, the extensive surface area of Ag NPs makes the NPs profitable antimicrobial agents[19]. Several Ag NPs were used against some gram-positive and gram-negative bacteria, they were jasmine flower extract synthesized Ag NPs against *Staphylococcus aureus and Escherichia coli* [7], *Alpinia nigra* fruits mediated Ag NPs against *Klebsiella pneumoniae*, *Staphylococcus aureus* and, *Candida albicans*[8], onion peels mediated Ag NPs mediated *Salmonella typhimurium* and *Staphylococcus aureus*[3], etc...

https://doi.org/10.36375/prepare_u.iiche.a379

In our study, *Livistona jekinsiana* and *Lasia spinosa* were applied in the synthesis of Ag NPs for the first time. Ag NPs were characterized by UV-Visible spectrophotometer, FTIR spectroscopy, XRD, SEM, TEM, EDS, XPS, DLS, and Zeta potential analysis. Ag NPs were used to inhibit the growth of microbes, *Escherichia coli*, *Pseudomonas aeruginosa*, *Staphylococcus aureus*, and *Candida albicans*. The aim of the evaluation of the antimicrobial activity of Ag NPs is to prepare herbal-based and cheap antimicrobial formulations for societal benefits. Ag NPs also possessed potential antioxidant, anti-inflammatory, and drug-delivery properties. These properties make Ag NPs cost-effective, biodegradable and biocompatible food packaging products. Moreover, all the biological properties helped in the development of new wound-healing Ag NPs based formulations. Ag NPs also efficiently degraded nitro compounds to valuable amino compounds followed by pseudo 1st order kinetics. Therefore, LJ and LS-assisted Ag NPs will be promising materials in the biomedical field, food packaging, and wastewater treatment.

2. Materials and Methods

All the chemicals used in each examination of the work were used as purchased. $AgNO_3$ was purchased from Merck and used as a precursor for the synthesis of Ag NPs. Mueller Hinton Agar and Broth (MHA & MHB), Potato Dextrose Agar and Broth (PDA & PDB), Neomycin, and Nystatin were used in the antimicrobial screening and purchased from Himedia. DPPH, Ascorbic Acid, Bovin Serum Albumin (BSA), Diclofenac, Ofloxacin, and C_2H_5OH were used in several biological screening of Ag NPs and were purchased from Himedia and Sigma-Aldrich. Nitro compounds were purchased from Merck and used in the screening of the photodegradation effect of NPs. Double distilled water (d. d. H_2O) was used as a solvent in the experiment.

2.1. Collection of plant materials and preparation of plant extracts

Livistona jekinsiana and *Lasia spinosa* were collected from Holmara village, Jorhat, Assam, India. Leaves of plants were washed with double distilled water to remove dust particles. Leaves were cut into small pieces, sun-dried, and ground into powder form. The powder of the leaves was stored in a zipper bag for further use.

10 g of each plant powder was added to an Erlenmeyer flask containing 100 ml d. d. H_2O. The mixture was stirred at 60^{o}C for 1 h and the extract was collected by filtration followed by centrifugation. The clear plant extract was stored at 4^{o}C for further application.

2.2. Livistona jekinsiana and Lasia spinosa assisted Ag NPs (LJ-Ag NPs and LS-Ag NPs)

3 mM of Ag NO_3 was added to 35 ml of plant extract in an amber-colored Erlenmeyer flask. The mixture was stirred for 3 h at 60^{o}C and the formation of Ag NPs was preliminarily confirmed by UV-Vis spectroscopy. The colloidal solution of Ag NPs was sonicated for 1 h to obtain well-dispersed NPs. After sonication, the NPs were collected by centrifugation at 5000rpm for 30 min thrice. The NPs were washed with d. d. H_2O to remove uncapped plant materials and dried at 75^{o}C for 24 h. The NPs were ground with mortar pestle and stored in a desiccator for different characterization and potential applications.

2.3. Antimicrobial Activity of LJ-Ag NPs and LS-Ag NPs

Antibacterial activity of the LJ-Ag NPs and LS-Ag NPs was studied against three bacterial strains and one fungal strain, *Escherichia coli* (ATCC 11229), *Staphylococcus aureus* (ATCC 11682), *Pseudomonas aeruginosa* (MTCC 2582), and *Candida albicans* (MTCC 3017). Mueller Hinton agar and Potato Dextrose agar were used as media in the agar well diffusion method for antibacterial and antifungal activity respectively. Selected microbes were cultured according to ATCC and MTCC protocols. With the help of a sterilized spreader, freshly cultured microbes were streaked on sterilized agar and a 6 mm well was made on agar by a sterilized borer. Different concentration of LJ-Ag NPs and LS-Ag NPs (20, 40, 60, 80, and 100 µg/ml) was added to the well. Neomycin and nystatin were used as a positive control in antibacterial and antifungal screening respectively. To observe the antimicrobial effects of Ag NPs on bacteria and fungi, NPs treated microbes were incubated at 37°C for 12 and 24 h for bacterial and fungal strains respectively. The zone of inhibition in mm was measured by the Antibiotic zone scale.

2.3.1. Minimum inhibitory concentration (MIC)

The broth dilution method was applied to determine the MIC of LJ-Ag NPs and LS-Ag NPs. Mueller Hinton Broth (MHB) and Potato Dextrose Broth (PDB) were used as media for bacteria and fungi respectively. Different concentrations (5, 15, 25, 35, 45, 55, 65, 75, 85, and 95µg/ml) of Ag NPs were added to 2 ml of freshly cultured microbes. The test tube filled with only broth and inoculums was considered a negative control. The test tubes were incubated for 24 h at 37^{o}C and 30^{o}C for 48 h for bacterial and fungal strains respectively. The minimum concentration of Ag NPs that inhibited the growth of microbes over 85% is considered as a MIC of LJ-Ag NPs and LS-Ag NPs.

2.4. Antioxidant Activity of LJ-Ag NPs and LS-Ag NPs

DPPH radical scavenging assay was applied to evaluate the antioxidant activity of LJ-Ag NPs and LS-Ag NPs. Antioxidants reduced DPPH (2, 2-diphenyl-1-picrylhydrazyl) to DPPHH. 2ml of different concentrations (20, 40, 60, 80 & 100µg/ml) of Ag NPs and positive control (ascorbic acid) were taken in test tubes. 1 ml of DPPH (.1mM of 20 ml ethanolic solution) solution was added to the stock solution. The absorbance of the mixture was measured at 517 nm against a 30% ethanolic aqueous solution. Only the DPPH solution was considered a negative control.

The DPPH free radical scavenging activity was calculated using the following formula:

% scavenging = [Absorbance of control - Absorbance of test sample/Absorbance of control] X 100

2.5. Anti-inflammatory activity of CCCLZF

The anti-inflammatory activity of LJ-Ag NPs and LS-Ag NPs was studied through in vitro assay. 5 ml of 0.2% w/v BSA was added to 50 ml of different concentrations of the NPs, heated at 72^{o}C for 5 min, and then cooled for 10 min. 5 ml of 0.2% w/v BSA solution with 50 ml water and Diclofenac (100 mg/ml) in water with 5 ml of 0.2% w/v BSA solution was considered as a control and standard respectively. The absorbance was measured at a wavelength

https://doi.org/10.36375/prepare_u.iiche.a379

of 276 nm and the result was interpreted in terms of the IC50 values.

2.6. Drug delivery action of LJ-Ag NPs and LS-Ag NPs

The drug delivery ability of LJ-Ag NPs and LS-Ag NPs was studied by considering ofloxacin as a model drug. The drug release behavior of Ag NPs was studied by UV-Vis spectroscopy. About 0.2 g of NPs was equilibrated in 20 ml of ofloxacin solution (100 ppm in distilled water) at 25°C for 2 days to load the drugs into the beads. Then, the solution was centrifuged, and the ofloxacin content was calculated using UV-Vis spectroscopy at 293 nm. The results of drug loading were calculated using the following equation.

% Drug Loading = (Weight drug in a sample/Weight of sample taken) X 100

The drug release profiles of Ag NPs were investigated at pH 7.4 for 24 h. In a typical experiment, 0.2 g of the drug-bearing NPs was placed in 10 ml of buffer solution (pH 7.4). The release medium was stirred at 37°C and 50 rpm. At the nominated time intervals, adequate amounts of samples were picked up and the number of released drugs was measured spectrophotometrically. The removed volume was replaced with a fresh buffer solution to maintain a constant volume of the test solution. The quantity of ofloxacin was determined using a standard calibration curve.

2.7. Photocatalytic Activity of LJ-Ag NPs and LS-Ag NPs

The photocatalytic activity of LJ-Ag NPs and LS-Ag NPs was evaluated by the reduction of 2-nitroaniline in presence of Ag NPs. 10 ml of 2-nitroaniline (0.1 mg/ml) and 10 ml Ag NPs (1mg/ml) were mixed and kept in dark condition for 30 min to attain adsorption-desorption equilibrium. The mixture was stirred at 37°C under solar irradiation and 2ml of aliquot was taken and centrifuged periodically with 10 min intervals. The photocatalytic degradation of 2-nitroaniline was monitored by a UV-Vis spectrophotometer between the ranges of 240 to 500 nm. The percentage of photocatalytic degradation of 2-nitroaniline was calculated using the following formulae.

Photocatalytic degradation (%) = (Co-Ct/Co) X 100

Co– Initial OD value of 2-nitroaniline (without Ag NPs),

Ct– OD value of Ag NPs treated nitro compounds.

3. Results and Discussion

3.1. Role of Livistona jekinsiana and Lasia spinosa extract in the synthesis of Ag NPs

Phytochemicals present in the plant extract play a major role in the synthesis and capping of NPs. Phenols, saponins, terpenoids, flavonoids, carbohydrates, proteins, tannins, steroids, anthraquinones, etc are present in the plant extracts of *Livistona jekinsiana* and *Lasia spinosa* [10,11]. These phytochemicals, especially polyphenolic compounds are responsible for the reduction of Ag+ ions to Ag (0) NPs. The development of NPs growth took place in two steps, 1st the reduction of Ag+ ions to Ag (0) by polyphenols than the capping of NPs by other phytochemicals[2]. The advantages of plant extracts in the synthesis of NPs are eco-friendly, cost-effective, time-economic, biocompatible, and lack harmful chemicals[9]. The selected plants have many traditional therapeutic applications in the treatment of various diseases[10,11]. These activities of the plant extracts made the LJ-Ag NPs and LS-Ag NPs efficient therapeutic agents for several diseases.

3.2. UV-Visible Spectra

The optical properties of the LJ-Ag NPs and LS-Ag NPs were studied by UV-Visible spectrophotometer. Both the NPs showed absorption maximum at 445 and 435 nm for LJ-Ag NPs and LS-Ag NPs respectively due to surface plasmon resonance [Fig. 1 (a)][6]. The absorption peaks at characteristic wavelengths resembled the literature and confirmed the formation of Ag NPs[8]. The single absorption peak determined the anisotropy of the NPs. The NPs were spherical and uniform in shape[20]. Higher surface plasmon resonance is responsible for the efficient photocatalytic activity of the Ag NPs[13].

3.3. FTIR Analysis

Surface constituents of LJ-Ag NPs and LS-Ag NPs were determined by FTIR analysis. FTIR spectra of Ag NPs confirmed the involvement of phytochemicals of *Livistona jekinsiana* and *Lasia spinosa* in the reduction of Ag+ ions to Ag (0) NPs and stabilization of NPs. The absorption bands at 3305 and 3450 cm^{-1} were observed in IR spectra of LJ-Ag NPs and LS-Ag NPs due to O-H stretching [Fig. 1 (b)][4]. The bands that appeared at 2836 and 2906 cm^{-1} showed the presence of C-H stretching[1]. Presence of amide I and amide II group in the surface of NPs was confirmed by the bond at 1637 cm^{-1} and 1560 cm^{-1} due to the C=O and –C-C- bond[1]. The bands appeared at 1390 and 1276 cm^{-1} assigned the C-C stretching and C-N stretching in aromatic ring[4]. Hence, phytochemicals especially polyphenols and carbonyl compounds of water extracts of leaves of selected plants responsible for synthesizing uniformly shaped and sized, and well-dispersed multifunctional Ag NPs.

3.4. XRD Analysis

The crystal structure properties of LJ-Ag NPs and LS-Ag NPs were determined by the XRD pattern of Ag NPs. The intense diffraction peaks appeared at 27.62°, 32.30°, 38.82°, 47.10°, 54.87°, 64.80°, and 77.20° could be related to the (210), (122), (111), (200), (142), (220) and (311) planes with the planes [Fig. 2 (a & b)][4,6]. These peaks resembled the previous data and confirmed the FCC structure of the Ag NPs[6]. The crystal structure of the Ag NPs was determined by Debye-Scherrer's equation

$$D = K\lambda/\beta \cos\theta$$

where D is the estimated crystallite size of Ag NPs, K is the Debye-Scherrer's constant, λ is the wavelength of the X-ray source, b is the angular width at the half maximum of the diffraction peak, and θ Bragg's angle. The estimated crystallite size of the LJ-Ag NPs and LS-Ag NPs were 22.35 and 25.46 nm respectively.

3.5. SEM Analysis

The morphology of the surface of the LJ-Ag NPs and LS-Ag NPs was analyzed by SEM micrographs at different magnifications. The uniform distribution of the monodispersed Ag NPs was revealed by the distributed white dots of SEM images [Fig. 3(a & b)]. The formation of deagglomerated Ag NPs by the biomolecules of *Livistona jekinsiana* and *Lasia spinosa* was confirmed by SEM images. The results were consistent with literature[6].

https://doi.org/10.36375/prepare_u.iiche.a379

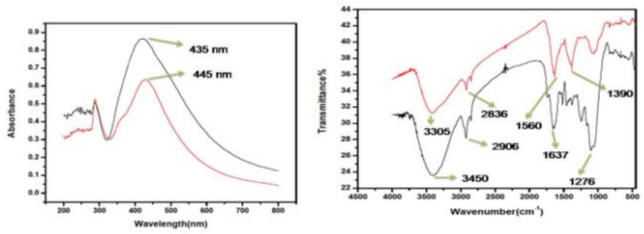

(a) (b)

Fig.1. (a) UV-Visible spectra of LJ-Ag NPs (red) and LS-Ag NPs (black); (b) FTIR spectra of LJ-Ag NPs (red) and LS-Ag NPs (black).

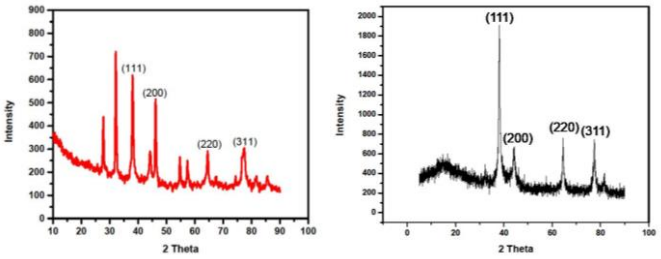

(a) (b)

Fig. 2. XRD pattern of LJ-Ag NPs (a) and LS-Ag NPs(b)

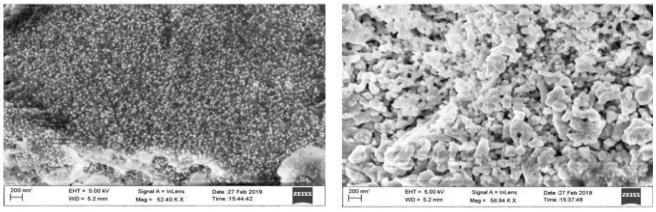

(a) (b)

Fig.3. SEM images of (a) LJ-Ag NPs; (b) LS-Ag NPs.

3.6. EDS Analysis

The elemental composition of the LJ-Ag NPs and LS-Ag NPs was determined by EDS analysis. The corresponding signal of Ag appeared at 3 keV due to surface plasmon resonance. Other signals of different atoms were also observed in the EDS spectra that revealed the presence of phytochemicals on the surface of the Ag NPs [Fig 4 (a & b)]. Atomic and weight percentages of different elements in the Ag NPs were also determined. The results resembled the reported data in literature[21].

(a)

Elements	Weight%	Atomic%
CK	62.78	88.79
NK	1.48	1.80
OK	4.18	4.44
AgL	31.56	4.97
Totals	100	

(b)

Elements	Weight%	Atomic%
CK	94.64	95.84
NK	1.35	1.17
OK	3.90	2.97
AgL	0.21	0.02
Totals	100	

Fig.4. EDS spectra of (a) LJ-Ag NPs; (b) LS-Ag NPs.

3.7. TEM, HRTEM and SAED Analysis

TEM analysis was applied to determine the shape and size of the LJ-Ag NPs and LS-Ag NPs. TEM images revealed that Ag NPs are spherical with no agglomeration. The size of the LJ-Ag NPs and LS-Ag NPs were 16.23 and 50 nm respectively calculated by Image J software. Lattice fringe spacing was 0.24 nm in HRTEM which corresponded to the (111) plane of the FCC crystal structure of Ag NPs [6]. Bright spots in the SAED pattern revealed the crystalline nature of the Ag NPs and (111) and (200) planes resembled the XRD pattern [Fig. 5 (a & b)]. The obtained data were consistent with literature [7].

3.8. Zeta Potential

The surface charge and stability of LJ-Ag NPs and LS-Ag NPs were determined by measuring the Zeta potential of Ag NPs. Zeta potentials of Ag NPs were found to be -23.1 mV and -25.9 mV [Fig. 6 (a & b)]. Negative zeta potential revealed the stability of the NPs and deagglomeration of the NPs. Phytochemicals successfully capped the NPs and made them useful for catalytic and biological applications[6,20].

DLS analysis determined the average hydrodynamic size of LJ-Ag NPs and LS-Ag NPs. The average sizes of LJ-Ag NPs and LS-Ag NPs were found to be 135.37 and 214.34 nm with polydispersity index of 0.813 and 0.186 respectively. The sizes obtained from DLS analysis were different from XRD and TEM due to the solvation effect[6,18].

3.9. Antimicrobial Activity

LJ-Ag NPs and LS-Ag NPs efficiently inhibited the growth of microbes. The graphical presentation of the antimicrobial activity of Ag NPs against, *E. coli*, *S. aureus*, *K. pneumonia*, and *C. albicans* was shown in Fig 7 and Fig. 8. The diameter of the inhibition zone of pathogens in the presence of LS-Ag NPs was illustrated in Table 1. It was observed that Ag NPs more efficiently inhibit the growth of gram-positive bacteria than gram-negative ones[4]. This was due to the different compositions of the cell wall of the gram-positive and gram-negative bacteria. The cell wall of gram-positive bacteria is composed of a thicker peptidoglycan layer but the cell wall of gram-negative bacteria is composed of a thinner peptidoglycan layer. Therefore, Ag NPs can easily penetrate through the cell membrane of the gram-negative bacteria and release Ag+ ions in the cytoplasm of the cell and causing cell death[4]. The mechanism of the antimicrobial actions of the Ag NPs is also based on the electrostatic interaction between the positive Ag NPs and gram-negative bacteria[4]. Extensive large surface area is also responsible for the excellent antimicrobial effects of the Ag NPs[4]. From Table 1, it was depicted that as the concentrations increased the antimicrobial activity of Ag NPs also increased. A larger amount of Ag NPs produced more reactive oxygen species (ROS) in the cell and destroyed all the cell organelles like DNA, mitochondria, ribosomes, enzymes, proteins, etc., and finally damaged the cell. The results of the antimicrobial activity of Ag NPs resembled the literature[4].

3.9.1. MIC of LJ-Ag NPs and LS-Ag NPs

MIC of Ag NPs was determined to estimate the minimum concentration of Ag NPs that inhibit the growth of microbes

https://doi.org/10.36375/prepare_u.iiche.a379

up to 85% [Table 2]. Lower MIC value of Ag NPs ascertained that the NPs will be a potential applicants in wound healing, treatment of urinary tract infection, etc.[4].

(a)

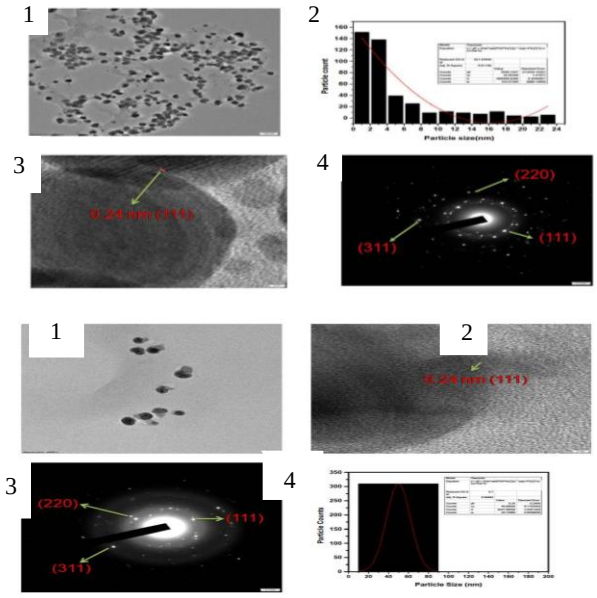

Fig.5. (a) TEM images (1), average particle size distribution (2), HRTEM (3) and SAED pattern (4) of LS-Ag NPs; (b) TEM images (1), HRTEM (2), SAED pattern (3) and average particle size distribution (d) of LJ-Ag NPs.

(a)

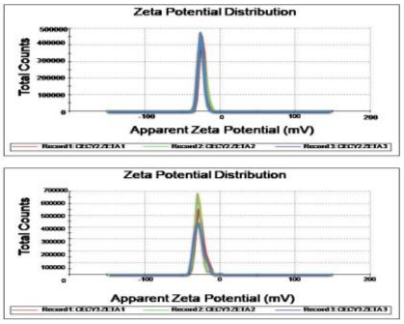

Fig.6. Zeta potential of (a) LJ-Ag & (b) LS-Ag NPs.

Table 2. MIC of LS-Ag NPs and LJ-Ag NPs.

3.10. Antioxidant Activity of LJ-Ag NPs and LS-Ag NPs

The antioxidant activity of the Ag NPs was determined by calculating the IC50 values of LJ-Ag NPs and LS-Ag NPs. The IC50 values were found to be 108.82 µg/ml, 241.14 µg/ml and 197.53 µg/ml for ascorbic acid, LJ-Ag NPs and LS-Ag NPs respectively [Fig. 9 (a)]. Lower IC50 values were due to the extra small size and the high surface-to-volume ratio of Ag NPs. The reduction of DPPH to DPPHH was described in Scheme 1 below. DPPH is a stable free radical in purple color. DPPH gets an electron from antioxidants and turns into yellowish DPPHH. Phytochemicals present on the surface of Ag NPs increased the antiradical property of the NPs. IC50 values resembled the previous data[4].

3.11. Anti-inflammatory Activity of LJ-Ag NPs and LS-Ag NPs

IC50 values of Ag NPs were found to be 422.71 µg/ml and 356.95 µg/ml for LJ-Ag NPs and LS-Ag NPs respectively. Diclofenac was considered a standard in the anti-inflammatory action of Ag NPs and the IC50 value of diclofenac was 331.23 µg/ml [Fig. 9 (b)]. The results were in agreement with the reported literature. Lower values of IC50 of Ag NPs concluded that Ag NPs will be a potential green alternative in the biomedical field[22].

3.12. Drug delivery action of LJ-Ag NPs and LS-Ag NPs

To evaluate the drug loading and drug release properties of LJ-Ag NPs and LS-Ag NPs, Ofloxacin was considered as a model drug. The drug loading capacity of LJ-Ag NPs and LS-Ag NPs was 32.78% and 35.34% respectively and encapsulation efficiency was 27.89% and 30.19% respectively. The drug-loading behavior of Ag NPs is due to the high surface area and extra small size of the NPs. *In vitro* drug release was performed in pH 7.4 PBS for 24h. The results were depicted in the calibration curve [Fig. 9 (c)].

3.13. Photocatalytic Activity of LJ-Ag NPs and LS-Ag NPs

Photocatalytic activity of the Ag NPs was evaluated by the reduction of 2-nitroaniline in the presence of LJ-Ag NPs and LS-Ag NPs. Ag NPs degraded the nitro compounds up to 87% following pseudo-1st-order kinetics with rate constant [Fig. 10 (a & b)]. The high surface area was the key factor for the efficient photocatalytic activity of Ag NPs[13]. A high surface area offers more active sites to adsorb the organic pollutants. The mechanism of the photodegradation of 2-nitroaniline was based on the electron-hole pair mechanism. Due to the high surface plasmon resonance of Ag NPs, electrons(e-) and holes(h+) require a longer time to recombine which is useful for photodegradation[13]. Electrons in the conduction band react with oxygen molecules to

S. No.	Test Organisms	Zone of Inhibition (in mm) for different concentrations (µg/ml) of LS-Ag NPs				Negative Control	Neomycin (Standard) (ZI)	Nystatin (Standard) (ZI)
		25	50	75	100			
1	*P. aeruginosa*	0	9± 0.4	11± 0.3	12± 0.6	0	19± 0.5	
2	*E. coli*	0	9± 0.0	10± 0.0	12± 0.2	0	20± 0.6	
3	*C. albicans*	9± 0.2	10± 0.2	11± 0.3	11± 0.9	0		22± 0.4
4	*S. aureus*	0	9± 0.2	10± 0.0	11± 0.2	0	22± 0.5	

Table 1. Antibacterial activity of LS-Ag NPs.

Microbial strains	MIC(µg/mL)	
	LS-Ag NPs	LJ-Ag NPs
P. aeruginosa	28	30
E. coli	32	34
C. albicans	28	32
S. aureus	36	38

https://doi.org/10.36375/prepare_u.iiche.a379

generate superoxide radical anion (O_2•−) and holes in the valance band react with surface-bound hydroxyl groups (OH−)[14]. Products of these reactions are free radicals and they can degrade nitro compounds or be reduced into environmentally friendly compounds[15]. Many reports were found in the literature on the reduction of nitrophenols but not for nitroaniline. Therefore, it is essential to reduce nitroaniline to diphenylamine which is a very useful starting material for the synthesis of several pharmaceutical compounds[16]. The results of the reduction of 2-nitro aniline in the presence of Ag NPs are consistent with the reported literature[17].

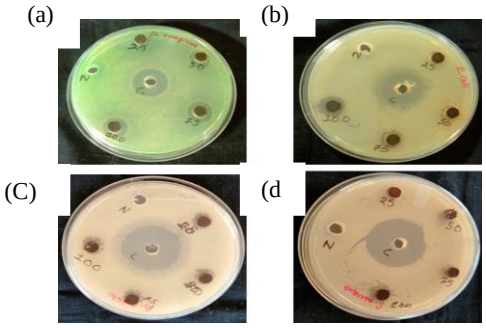

Fig. 7. Inhibition zone of (a) PA, (b) EC, (c) CA, and (d) SA in the presence of LS-Ag NPs.

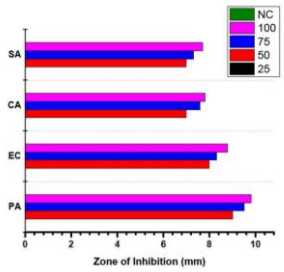

Fig. 8. Inhibition zone of (a) PA, (b) EC, (c) CA, and (d) SA in the presence of LJ-Ag NPs.

Conclusion

Livistona jekinsiana and *Lasia spinosa*-mediated Ag NPs were synthesized using eco-friendly and cost-effective methods. Ag Nps were characterized by UV-Visible and FTIR spectroscopy, XRD, SEM, EDS, TEM, XPS, DLS, and zeta potential analysis. UV-Visible peaks at 445 and 435 nm revealed the high surface plasmon resonance of Ag NPs that was useful for photocatalytic applications. FTIR, EDS, and XPS analysis confirmed the presence of Ag NPs along with phytochemicals in NPs. SEM and TEM analysis showed the formation of deagglomerated NPs that was essential for their catalytic and biological application. The high negative value of the zeta potential of Ag NPs made them efficient applicants in various fields. LS-Ag NPs showed better biological application than LJ-Ag NPs due to the bioactive compound present in the extracts of *Lasia spinosa*. Therefore, synthesized Ag NPs will be efficient therapeutic applicants in urinary tract infections, wound healing, and remedial agents in wastewater management.

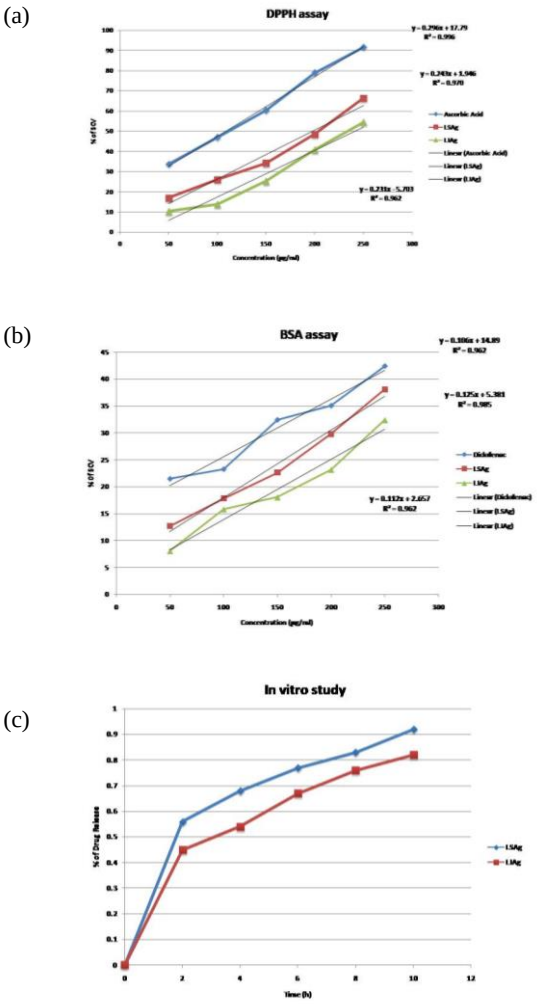

Fig. 9. (a) Antioxidant activity; (b) anti-inflammatory activity; (c) drug releasing property of LS-Ag NPs and LJ-Ag NPs.

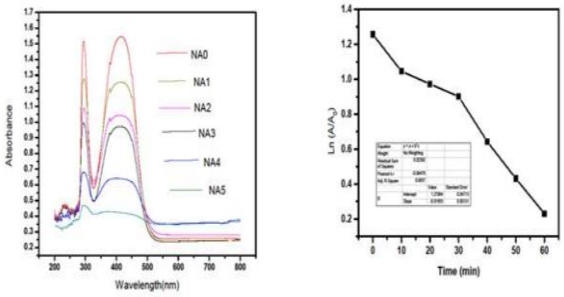

(a) (b)

Fig. 10. (a) Photocatalytic degradation of 2-nitroaniline; (b) kinetics of the degradation in the presence of LS-Ag NPs.

Acknowledgment

The authors were heartily grateful to the Director of CSIR-NEIST for his guidance and for permitting us to carry out our research in his institute with excellent facilities. R.B.

was also thankful to the Department of Science and Technology, New Delhi, for the Fellowship [DST-INSPIRE, GAP-0754].

References

(1) Manik, U. P.; Nande, A.; Raut, S.; Dhoble, S. J. Green synthesis of silver nanoparticles using plant leaf extraction of Artocarpus heterophylus and Azadirachta indica. Result. Mater. 2020, 6, 100086.

(2) Ahmed, S.; Ahmed, M.; Swami, B. L.; Ikram, S. A review on plants extract mediated synthesis of silver nanoparticles for antimicrobial applications: A green expertise. J. Adv. Res. 2016,7, 17–28.

(3) Santhosh, A.; Theertha, V.; Prakash, P.; Chandran, S. S. From waste to a value added product: Green synthesis of silver nanoparticles from onion peels together with its diverse applications. Mater. Today: Proc. 2021, 46, 4460–4463.

(4) Jalilian, F.; Chahardoli, A.; Sadrjavadi, K.; Fattahi, A.; Shokoohinia, Y. Green synthesized silver nanoparticle from *Allium ampeloprasum* aqueous extract: Characterization, antioxidant activities, antibacterial and cytotoxicity effects. Adv. Powder Technol. 2020, 31, 1323-1332.

(5) Yuan, Z.; Yang, H.; Xu, P.; Li, C.; Jian, J.; Zeng, J.; Zeng, L.; Sui, Y.; Zhou, H. Facile in situ synthesis of silver nanocomposites based on cellulosic paper for photocatalytic applications. Environ. Sci. Pollut. Res. 2021, 28, 6411-6421.

(6) Baruah, D.; Yadav, R. N. S.; Yadav, A.; Das, A. M. *Alpinia nigra* fruits mediated synthesis of silver nanoparticles and their antimicrobial and photocatalytic activities. J. Photochem. Photobiol. B Biol. 2019, 201, 111649.

(7) Baruah, R.; Yadav, A.; Das, A.M. Evaluation of the multifunctional activity of silver bionanocomposites in environmental remediation and inhibition of the growth of multidrug-resistant pathogens† New J. Chem., 2022, 46**,** 10128-10153.

(8) Chandhirasekar, K.; Thendralmanikandan, A.; Thangavelu, P.; Nguyen, B. S.; Nguyen, T. A. Sivashanmugan, K.; Nareshkumar, A.; Nguyen, V. H. Plant-extract-assisted green synthesis and its larvicidal activities of silver nanoparticles using leaf extract of *Citrus medica*, *Tagetes lemmonii*, and *Tarenna asiatica*. Mater. Lett. 2021, 287, 129265.

(9) Abdullah, H. S. T. S. H.; Asseri, S. N. A. R. M.; Mohamad, W. N. K. W.; Kan, S. Y.; Azmi, A. A.; Julius, F. S. Y.; Chia, P. W. Green synthesis, characterization and applications of silver nanoparticle mediated by the aqueous extract of red onion peel☆ Environ. Pollut. 2021, 271, 116295.

(10) Singh, R. K.; Srivastava, R. C.; Mukherjee, T. K. *Toko-Patta* (*Livistona jenkinsiana* Griff): *Adi* community and conservation of culturally important endangered tree species in eastern Himalaya. Indian J. Tradit. Knowl. 2010, 9, 231-241.

(11) Brahma, J.; Chakravarty, S.; Rethy, P. Qualitative Estimation of the Presence of Bioactive and Nutritional Compound in Lasia Spinosa: An Important Vegetable Plant used by the Bodos of Kokrajhar District. Int. J. Chemtech Res. 2014, 6, 1405-1412.

(12) Albukhari, S. M.; Ismail, M.; Akhtar, K.; Danish, E. Y. Catalytic reduction of nitrophenols and dyes using silver nanoparticles @ cellulose polymer paper for the resolution of waste water treatment challenges. Colloids Surf. A Physicochem. Eng. Asp. 2019, 577, 548-561.

(13) Yuan, Z.; Yang, H.; Xu, P.; Li, C.; Jian, J.; Zeng, J.; Zeng, L.; Sui, Y.; Zhou, H. Facile in situ synthesis of silver nanocomposites based on cellulosic paper for photocatalytic applications. Environ. Sci. Pollut. Res. 2021, 28, 6411-6421.

(14) Lee, S. J.; Begildayeva, T.; Yeon, S.; Naik, S. S.; Ryu, H.; Kim, T. H.; Choi, M. Y. Eco-friendly synthesis of lignin mediated silver nanoparticles as a selective sensor and their catalytic removal of aromatic toxic nitro compounds☆ Environ. Pollut. 2021, 269, 116174.

(15) Zhu, D.; Long, L.; Sun, J.; Wan, H.; Zheng, S. Highly active and selective catalytic hydrogenation of *p*-chloronitrobenzene to *p*-chloroaniline on Pt@Cu/TiO_2. Appl. Surf. Sci. 2020, 504, 144329.

(16) Karthik, R.; Govindasamy, M.; Chen, S. M.; Cheng, Y. H.; Muthukrishnan, P.; Padmavathy, S.; Elangovan, A. Biosynthesis of silver nanoparticles by using *Camellia japonica* leaf extract for the electrocatalytic reduction of nitrobenzene and photocatalytic degradation of Eosin-Y. J. Photochem. Photobiol. B Biol. 2017, 170, 164-172.

(17) Cynthia, G.; Swarnavalli, J.; Dinakaran, S.; Krishnaveni, S.; Bhalerao, G. M. Rapid one pot synthesis of Ag/ZnO nanoflowers for photocatalytic degradation of nitrobenzene. Mater. Sci. Eng. B 2019, 247, 114376.

(18) Dutta, T.; Ghosh, N. N.; Das, M.; Adhikary, R.; Mandal, V.; Chattopadhyay, A. P. Green synthesis of antibacterial and antifungal silver nanoparticles using *Citrus limetta* peel extract: Experimental and theoretical studies. J. Environ. Chem. Eng. 2020, 8, 104019.

(19) Shah, Z.; Gul, T.; Khan, S. A.; Shaheen, K.; Anwar, Y.; Suo, H.; Ismail, M.; Alghamdi, K. M.; Salman, S.M. Synthesis of high surface area AgNPs from *Dodonaea viscosa* plant for the removal of pathogenic microbes and persistent organic pollutants. Mater. Sci. Eng. B 2021, 263, 114770.

(20) Baruah, R.; Yadav, A.; Das, A. M. *Livistona jekinsiana* fabricated ZnO nanoparticles and their detrimental effect towards anthropogenic organic pollutants and human pathogenic bacteria. Spectrochim. Acta A Mol. Biomol. Spectrosc. 2021, 251, 119459.

(21) Ugwoke, E.; Aisida, S. O.; Mirbahar, A. A.; Arshad, M.; Ahmad, I.; Zhao, T., Ezema, F. I. Concentration induced properties of silver nanoparticles and their antibacterial study. Surf. Interfaces 2020, 18, 100419.

(22) Kumar, V.; Singh, S.; Srivastava, B.; Bhadouria, R.; Singh, R. Green synthesis of silver nanoparticles using leaf extract of *Holoptelea integrifolia* and preliminary investigation of its antioxidant, anti-inflammatory, antidiabetic and antibacterial activities. J. Environ. Chem. Eng. 2019, 7, 103094.